Agricultural Water Management 115 (2012) 83–91

Contents lists available at SciVerse ScienceDirect

Agricultural Water Management

journal homepage: www.elsevier.com/locate/agwat

Development of Variable Threshold Models for detection of irrigated paddy rice fields and irrigation timing in heterogeneous land cover

S. Jeong [a], S. Kang [a,*], K. Jang [a], H. Lee [b], S. Hong [c], D. Ko [d]

[a] Department of Environmental Science, Kangwon National University, Chuncheon 200-701, Republic of Korea
[b] Department of Geophysics, Kangwon National University, Chuncheon 200-701, Republic of Korea
[c] Soil and Fertilizer Management Division, National Academy of Agriculture Science, Rural Development Administration, Suwon 441-707, Republic of Korea
[d] Department of Forest, Environment, and Systems, Kookmin University, Seoul 136-702, Republic of Korea

ARTICLE INFO

Article history:
Received 25 February 2012
Accepted 23 August 2012

Keywords:
Satellite data
Spectral index
Surface water detection
Sub-pixel heterogeneity

ABSTRACT

Accurate monitoring of irrigated paddy field area and irrigation timing are of a great concern in agricultural water management due to the substantial consumption of fresh water when irrigating paddy fields. Spectral threshold methods (Xiao et al., 2005) have been widely applied to detect irrigated paddy fields and irrigation timing using Moderate Resolution Imaging Spectroradiometer (MODIS) Enhanced Vegetation Index (EVI) and Land Surface Water Index (LSWI). These methods applied constant additive threshold values (T) to LSWI and compared it to EVI to detect the irrigated paddy fields. In this study, we developed Variable Threshold Models that utilized different pixel-based threshold values depending on sub-pixel land cover heterogeneity and hence, improve detection performance on distributed small-scale paddy fields. Non-irrigated sub-pixels were quantified with irrigation maps produced by Synthetic Aperture Radar (SAR) microwave images. Significant positive correlation between EVI and the sub-pixel numbers of non-irrigated area were found ($r = 0.87$), which resulted in higher T for MODIS pixels with more non-irrigated sub-pixels. Accordingly, a Variable Threshold Model, i.e. a regression model between T and EVI, was developed. With the Variable Threshold Model, agreement rates between MODIS and SAR-based irrigated small-scale paddy field classification doubled compared with that from a fixed threshold value. In comparison with field observations, the Variable Threshold Models showed a mean error of +0.9 days, an improvement over the mean error of +2.8 days from a fixed threshold model. Combined utilization of SAR and MODIS images provides a useful tool for developing a Variable Threshold Model that can enhance accurate monitoring of irrigation dates across heterogeneous paddy field regions.

1. Introduction

Rice is one of world's major food resources, supporting more than 50% of the world population (Bouvet and Toan, 2011). The area covered by paddy rice fields has increased by +80 M ha yr^{-1} (UNDESA, 2004), which may lead to increased demands for fresh water to irrigate new paddy rice fields. Such increased demand may result in water resource problems in water-limited areas. Irrigation of paddy fields in Asia accounts for approximately 70% of fresh water outflows (Samad et al., 1992), and in some Asian countries over 95% of fresh water is used for irrigation (FAOSTAT, 2001; Xiao et al., 2006). Paddy field irrigation can also enhance evapotranspiration, which may result in an imbalance of local and regional water budgets. Hence, reliable monitoring of irrigation timing is an important concern in areas with insufficient water resources.

Satellite remote sensing has been utilized as a useful alternative means for monitoring irrigated area and irrigation timing over large areas, because acquiring irrigation data is highly limited in many countries and partially available only for administrative management units (Ozdogan et al., 2010). Since Moderate Resolution Imaging Spectroradiometer (MODIS) images have been available since 2000, there has been considerable progress in estimating the spatial distribution of irrigated fields (Xiao et al., 2005; Sakamoto et al., 2007; Sun et al., 2009; Gumma et al., 2011) and the timing of irrigation using the MODIS spectral indices (Jeong et al., 2011; Peng et al., 2011).

Xiao et al. (2005) proposed a simple threshold algorithm to detect paddy rice fields using MODIS EVI (Enhanced Vegetation Index), NDVI (Normalized Difference Vegetation Index), and LSWI (Land Surface Water Index). EVI and NDVI are vegetation indices sensitive to vegetation greenness and biomass, while LSWI is a

* Corresponding author. Tel.: +82 33 250 8578; fax: +82 33 251 3991.
E-mail address: kangsk@kangwon.ac.kr (S. Kang).

0378-3774/$ – see front matter © 2012 Elsevier B.V. All rights reserved.
http://dx.doi.org/10.1016/j.agwat.2012.08.012

spectral index sensitive to moisture content of the land surface. Any MODIS pixel meeting the condition, LSWI + $T \geq$ EVI (or NDVI), was identified as a paddy rice field. Here, T is a constant additive threshold value.

The threshold algorithm was based on their findings in southern China and Southeast Asia, from which paddy rice fields showed higher LSWI values than NDVI (or EVI) during the period of irrigating or transplanting. Compared to their earlier study (Xiao et al., 2002), they applied a constant additive threshold (T = 0.05) for LSWI to slightly relax the condition of the difference between LSWI and EVI (or NDVI) for irrigation detection because green non-irrigated sub-pixels can cause higher EVI (or NDVI) compared to pure irrigated paddy field pixels during irrigation periods. Although threshold (T) enhanced detection of irrigated paddy fields and timing was introduced, there were still several problems caused by background reflectance from other components such as ditches, roads, other crops, temporal mixing of irrigation caused by early and late transplanting, and single or multiple cropping.

Sun et al. (2009) and Peng et al. (2011) separated the planted area based on rice cropping systems and modified the threshold (T) accordingly: rice fields were separated into early and late rice fields. The improvements from this approach were most distinguishable in detecting irrigated area and irrigation timing of large-scale paddy fields, but significant uncertainty still remained in regions with highly distributed small-scale paddy fields. Jeong et al. (2011) applied the irrigation detection algorithm suggested by Xiao et al. (2005) and Peng et al. (2011) in the Republic of Korea with mixed results: irrigated areas were overestimated for regions with large-scale paddy rice fields, while those with small-scale paddy rice fields were underestimated. Similar uncertainties were also reported by other studies using the method of Xiao et al. (2005), especially for the small-scale paddy field regions (Uchida, 2007; Islam et al., 2010). A major cause of such uncertainties is the background reflectance from green non-irrigated sub-pixels within a MODIS EVI pixel (Sun et al., 2009; Jeong et al., 2011). The green non-irrigated portion tends to increase MODIS EVI (or NDVI) during the irrigation period, which subsequently requires a higher threshold (T) to detect the paddy field irrigation.

Reliable information on the counts of irrigated and non-irrigated sub-pixels is required to determine the effects of non-irrigated sub-pixels on MODIS spectral indices and hence, to determine the appropriate threshold (T) to minimize uncertainty from the mixed-pixel problem. Synthetic Aperture Radar (SAR) satellite imaging is a useful tool for differentiating irrigated paddy fields from other landforms and non-irrigated paddy rice fields because of its high sensitivity to surface water (Lee, 2006; Islam et al., 2010). In addition, the higher spatial resolution of SAR image compared to MODIS enables quantification of sub-pixel heterogeneity, assessment of its effect on the MODIS spectral indices, and analysis of errors caused by using coarse resolution MODIS images in determining the irrigation timing and the irrigated paddy rice fields (Park et al., 2005; Sakamoto et al., 2007).

In this study, the MODIS-based irrigation detection algorithm proposed by Xiao et al. (2005) was improved, with the particular purpose of reducing detection uncertainty caused by distributed small-scale paddy field regions. Our approach utilized SAR-based irrigated paddy field maps to develop the Variable Threshold Model for the threshold (T) in conjunction with MODIS EVI.

2. Materials and methods

2.1. Study area and land cover characteristics

The development of the Variable Threshold Model was conducted in the Yedang wide plains located in the mid-west of the Republic of Korea. Both large and small-scale paddy fields are mixed within the extent of each available Radarsat-1 SAR image (Fig. 1). The annual average temperature and the annual total precipitation of this region ranged from 10 to 16 °C and 1000 to 1800 mm, respectively. Based on the National Land Cover Map (5 m resolution, produced by Ministry of Environment of Korea), 64.2% of the region is covered with forest, 10% by paddy rice fields, 8.3% by dry crop fields, and 17.5% by other land cover classes.

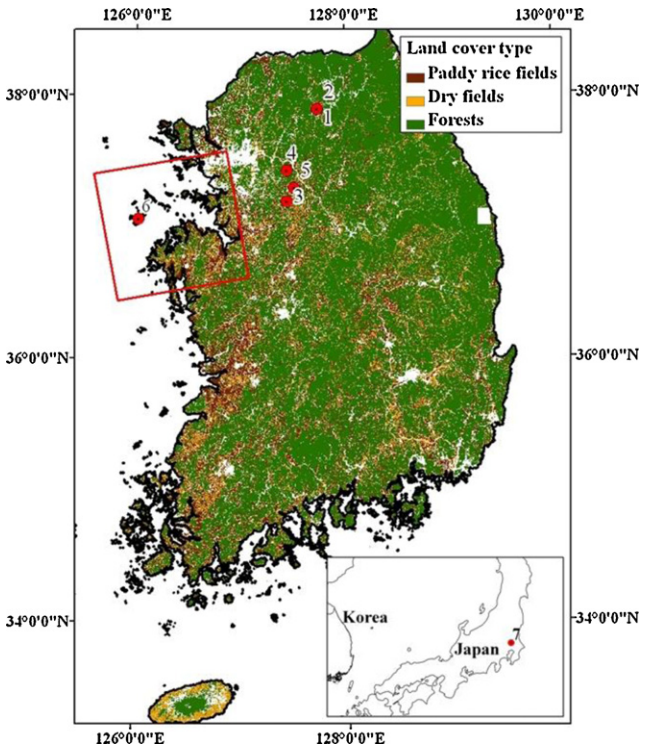

Fig. 1. Main land cover map of raster form (20 m) developed by the Ministry of Environment in the Republic of Korea. The square is the test area used to determine the error factor from land cover heterogeneity.

The validation of the Variable Threshold Model was based on six sites in Korea and one site in Japan, where field observation data on irrigation dates and field photos were available between 2001 and 2010 (Moon et al., 2003; Lee et al., 2005) (Table 1). As a final step, the Variable Threshold Model to the entirety of South Korea was applied to examine the spatial variation of irrigation dates.

Previous studies using the threshold method tried to detect both paddy field area and irrigation date, and hence, they developed their own MODIS-based paddy field maps that contain some uncertainties in the classification process. However, since the primary concerns were the improvement of the MODIS-based detection performance of distributed small-scale paddy rice fields and irrigation timing, the study was confined to only predetermined paddy rice areas that were extracted from the National Land Cover Map. The National Land Cover Map was aggregated into 20 m and 500 m resolution land cover maps to meet the spatial scales of SAR and MODIS, respectively. In the aggregation process, sub-pixel numbers for rice paddies, dry crop fields, and forests within a 500 m MODIS pixel were counted separately, which was later utilized to examine the relationships between MODIS spectral indices and sub-pixel land cover heterogeneity.

2.2. Data collection and manipulation

Two types of satellite images were collected in this study: two radarsat-1 SAR images from 2003 and MODIS 8-day reflectance products from 2001 to 2010. By producing 20 m resolution maps

Table 1
General information on the evaluation sites of the Variable Threshold Model.

Site number	Site name	Location	Annual mean temperature (°C)	Annual mean precipitation (mm)	Data year	Irrigation period (DOY)
1	ChoonCheon1 (Korea)	37°54′ 15.18″N, 127°43′ 55.58″E	10.9	1266	2010	120–150
2	ChoonCheon2 (Korea)	37°54′ 16.89″N, 127°44′ 03.7″E			2010	125–130
3	Icheon1 (Korea)	37°12′ N, 127°26′ 37.8″E			2010	117–131
4	Icheon2 (Korea)	37°26′ 05.8″N, 127°26′ 34.4″E	11.2	1329	2010	121–131
5	Icheon flux (Korea)	37°18′ 20.34″N, 127°30′ 40.46″E			2003	120–131
6	Hari flux (Korea)	37°4′N, 126°2′E	10.8	1139	2002	126–130
7	MASE flux (Japan)	36°03′ 14.3″N, 140°01′36.9″E	13.7	1200	2001–2004	108–124

of irrigated paddy fields, the SAR images were utilized to estimate the fraction of irrigated and non-irrigated portions within a MODIS pixel. Two spectral indices, EVI and LSWI, were calculated from the MODIS reflectance products, which were applied to determine irrigated pixels and irrigation timing.

2.2.1. Radarsat-1 SAR images

Radarsat-1 SAR images taken on May 6 (day of year [DOY] 126) and May 30 (DOY 150) in 2003 were collected for the Yedang wide plains (Fig. 2). Radarsat-1 SAR images have a spatial resolution of 20 m, and record backscattering radiation at a wavelength of 5.6 cm (C-band) with an incidence angle of 39°. A two-step data processing for the SAR images was performed to produce reference maps of irrigated paddy fields. First, the paddy rice fields identified in the Korea Land Cover Map were extracted from the SAR images. Second, for the extracted SAR pixels only, supervised classification was implemented to identify the irrigated paddy fields with a training dataset determined by visual interpretation of irrigated paddy fields. Based on the SAR irrigation maps, the number of irrigated SAR pixels was recorded for every 500 m MODIS pixel to produce irrigation count maps with a spatial resolution identical to MODIS EVI.

2.2.2. MODIS EVI and LSWI

This study used Terra MODIS 8-day composite surface reflectance products (MOD09A1) from 2001 to 2010. The 500 m resolution reflectance data from blue (ρ_{blue}, 459–479 nm), red (ρ_{red}, 620–670 nm), near infrared (ρ_{nir}, 841–875 nm), and shortwave infrared (ρ_{swir}, 2105–2155 nm) were utilized to calculate EVI and LSWI:

$$\mathrm{EVI} = \frac{\rho_{nir} - \rho_{red}}{\rho_{nir} + 6\rho_{red} - 7.5\rho_{blue} + 1} \quad (1)$$

$$\mathrm{LSWI} = \frac{\rho_{nir} - \rho_{swir}}{\rho_{nir} + \rho_{swir}} \quad (2)$$

EVI rather than NDVI was preferred because EVI reduces soil reflectance and atmospheric contamination, and enhances sensitivity to highly vegetated areas (Huete et al., 1997, 2002). This feature makes EVI more appropriate than NDVI since adjacent forest patches show considerable greening by May when irrigation reaches its peak in Korea. LSWI is a vegetation index sensitive to moisture content of the land surface.

The MOD09A1 product provides quality assurance (QA) information on the selection of data processing method, presence of cloud cover, etc. To minimize the error associated with cloud

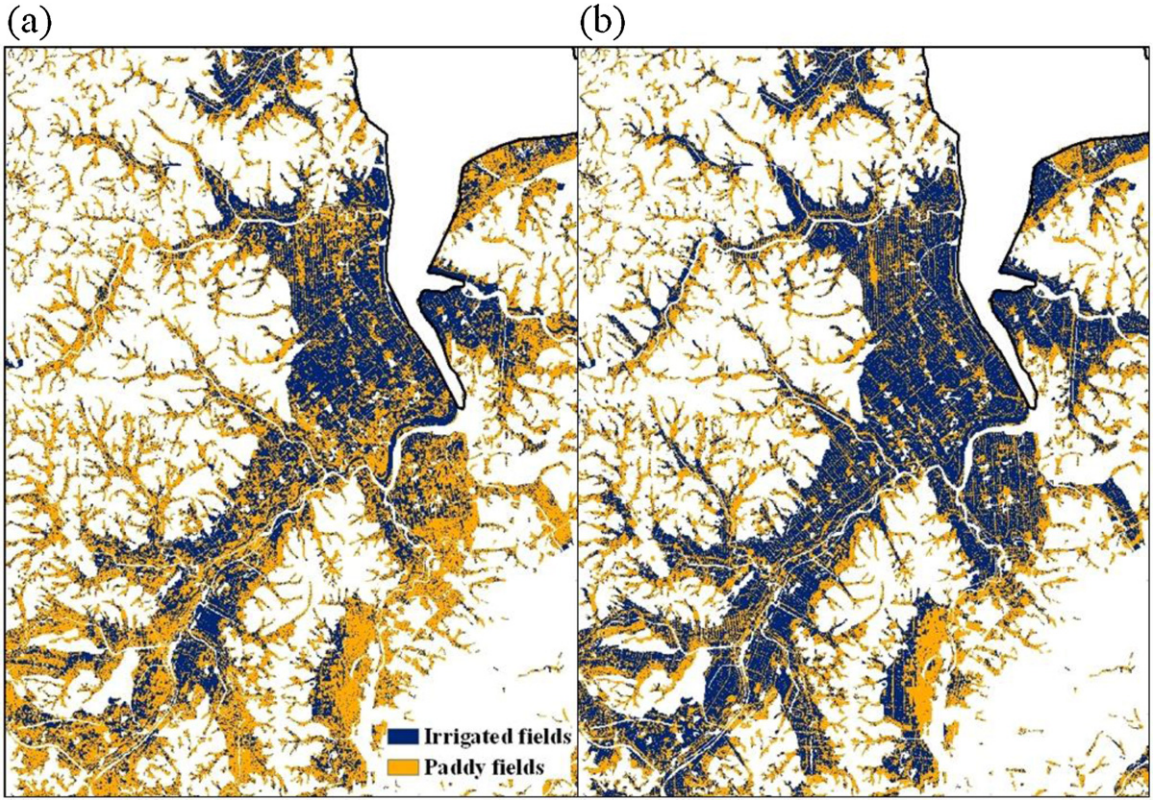

Fig. 2. SAR-based irrigated paddy rice fields obtained using the supervisor classification method in DOY 126 (a) and in DOY 150 (b).

or aerosol contamination, we discarded MOD09A1 data with either/both poor QA or/and blue reflectance greater than or equal to 0.2, an indication of cloudy pixels (Xiao et al., 2005; Sakamoto et al., 2007). In such cases, the discarded data was replaced with the mean value of previous and subsequent available reflectance data.

2.3. Development of variable threshold model

The irrigation detection algorithm, LSWI + $T \geq$ EVI, developed by Xiao et al. (2005) was applied. They proposed a threshold value (T) of 0.05, which was used by studies such as Sakamoto et al. (2007), Islam et al. (2010), and Jeong et al. (2011) to make the inundation (or paddy rice fields) maps. Sun et al. (2009) and Peng et al. (2011) modified the T value to reflect the biophysical characteristics of their local study sites. All of the studies used fixed T values for their study areas. In this study, however, it was hypothesized that the T value would be variable depending on the sub-pixel fraction of non-irrigated landforms based on the following reasons.

In the irrigation detection algorithm, T plays a determinant role in the detection accuracy. If T is too high, irrigated paddy field area could be overestimated because the irrigation condition can be met with lower LSWI and consequently, the estimated timing of irrigation becomes earlier than true irrigation. Basically, T represents different spectral characteristics for LSWI and EVI on mixed land cover pixels. LSWI is very sensitive to and rapidly saturated with the irrigated sub-pixels, but is less sensitive to sub-pixel greenness than EVI. For example, for a pixel with higher greenness, it will show increased EVI while LSWI will remain at a similar level, and therefore a higher T value is necessary to detect sub-pixel irrigation. Therefore, one may be able to improve irrigation detection by using variable T values depending on the greenness of non-irrigated sub-pixels within a MODIS pixel. In this study, EVI was assumed to be a useful spectral index representing the greenness of non-irrigated sub-pixels and then, hypothesized that T is positively linearly related to EVI.

$$T = \alpha \cdot \mathrm{EVI} + \beta \quad (3)$$

where α and β are empirical regression coefficients relating EVI with T.

To develop the Variable Threshold Model (Eq. (3)), it was first investigated which spectral index is better related with the number of non-irrigated sub-pixels. Consequently, EVI was identified as the superior index, showing a higher correlation coefficient ($r = 0.87$) with the number of non-irrigated sub-pixels than LSWI ($r = 0.49$). Second, we determined the T value for every MODIS pixel by increasing T from 0.0 at an interval of 0.01 until the irrigation condition as described in Eq. (1) was satisfied. Finally, the regression model (Eq. (3)) was developed by using EVI and the determined T value.

One of the potential problems of this method occurs when forest sub-pixels are dominant over paddy or dry fields. Because of the very high level of EVI for forest sub-pixels, the T value in MODIS pixels dominated by forests becomes extremely high, resulting in early irrigation timing and over-estimation of the irrigated fields. To overcome this problem, we limited the maximum T to the highest T value found in MODIS pixels dominated by either paddy or dry fields.

The Variable Threshold Model was applied to specify the threshold (T) of each pixel and the timing of irrigation was determined as the first date of the EVI 8-day period that meets the irrigation detection condition.

2.4. Statistical analysis

Agreement rate between 500 m MODIS and 20 m SAR-derived irrigation maps was calculated to test model performance on detection of the irrigated paddy fields for the dates of the two SAR images. The agreement rate is calculated as the percent of SAR irrigation pixels contained in MODIS irrigation pixels to total SAR irrigation pixels. We calculated the agreement rate for six different classes of irrigated sub-pixel numbers (i.e. less then 100, 200, 300, 400, 500, and over 500) to investigate model performance depending on sub-pixel heterogeneity. The agreement rate was expected to increase with the irrigated sub-pixel numbers because of the prevailing effect of irrigated sub-pixels on both MODIS EVI and LSWI. Hence, the model adaptability was primarily determined based on how well the model can detect irrigation for low irrigated sub-pixel classes.

The detected timing of irrigation was evaluated with the irrigation data collected from field observations between 2001 and 2010 (Table 1). The MODIS-based irrigation was evaluated every 8 days and the first detection date was designated as the irrigation date.

3. Results

3.1. Relationships between vegetation indices and sub-pixel heterogeneity

For the SAR image area, mean sub-pixel counts for irrigated paddy field, dry field, and forest land covers were compared with MODIS EVI and LSWI for the two SAR images (Fig. 3). The histograms of LSWI showed a highly mixed pattern, and it was difficult to find a trend to differentiate each of the land cover types (Fig. 3a and b). In contrast, EVI histograms showed clear differences, with decreasing, uni-modal, and increasing patterns for irrigated paddy field, dry field, and forest, respectively (Fig. 3c and d). Low EVI values for most of the irrigated paddy fields indicate that MODIS pixels with prevailing irrigated paddy field sub-pixels have very limited vegetation growth on the dates of SAR images. As the proportion of irrigated paddy fields decreases, the EVI increases subsequently. This implies that a higher T value is necessary to detect irrigation of such MODIS pixels. Since forest shows considerable growth by May, EVI gradually increases with the proportion of forest sub-pixels, while grassy type vegetation in dry fields showed maximum counts around 0.2–0.3 EVI.

3.2. Developing variable threshold (T) model

For every MODIS pixel, the threshold (T) was identified as the first T value when the irrigation condition, LSWI + $T \geq$ EVI, was satisfied for each SAR images date. Then, we developed regression models (Eq. (3)) between EVI and the areal mean T of the SAR image extent. Three alternative regression models were developed by using single and composite SAR images, respectively:

$$T1 = 0.5500 \cdot \mathrm{EVI} + 0.0061\,(\mathrm{DOY}\,126) \quad (4)$$

$$T2 = 0.3881 \cdot \mathrm{EVI} - 0.0043\,(\mathrm{DOY}\,150) \quad (5)$$

$$T3 = 0.4236 \cdot \mathrm{EVI} + 0.0112\,(\mathrm{composite\ dates}) \quad (6)$$

here, $T1$, $T2$, and $T3$ are the threshold T values of DOY 126, DOY 150, and composite dates, respectively. For all cases, the areal mean T showed strong positive correlations with EVI ($r > 0.99$). To prevent an overly high T value, which will result in overestimation of irrigated area, we set allowable maximum T at EVI where dry fields are more dominant than forest sub-pixels. The EVI was identified as 0.24, 0.32, and 0.28 for the DOY 126, DOY 150, and composite SAR images, respectively, which corresponded with maximum T values of 0.14, 0.13, and 0.13, respectively.

Fig. 5 demonstrates the effect of variable T values on detection of small-scale irrigated paddy fields on DOY 126. The results of using

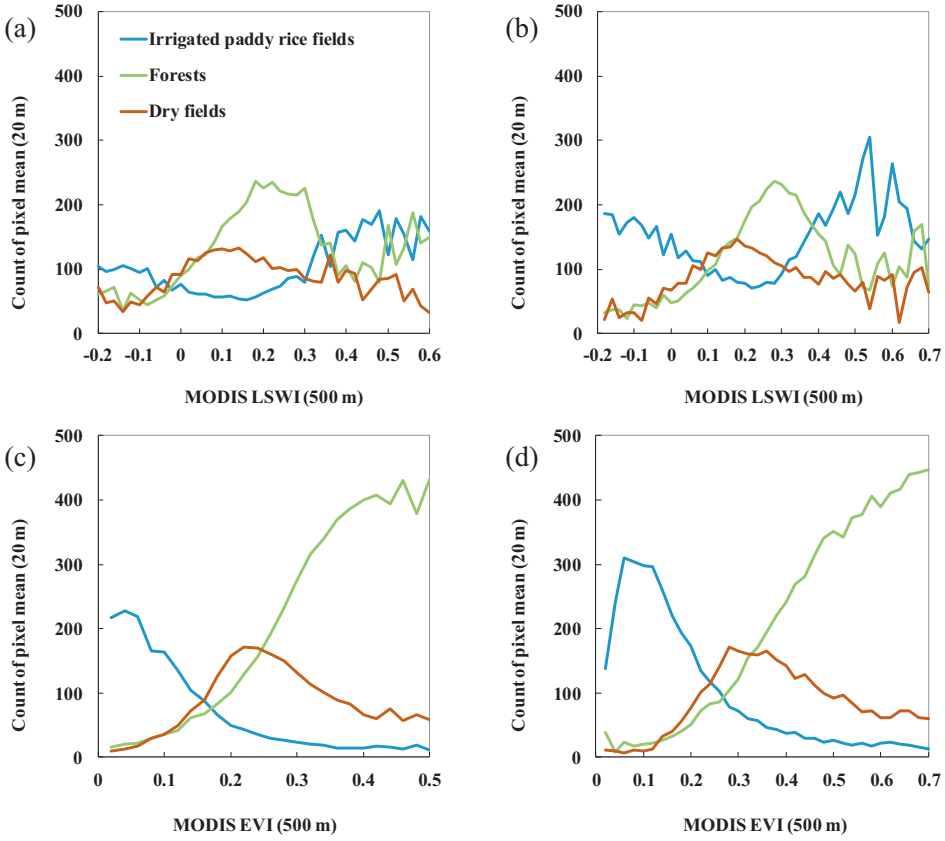

Fig. 3. Counts of land cover pixels (irrigated paddy rice fields, forests, and dry fields) with MODIS-based LSWI (a, b) and EVI (c, d) for SAR image dates of DOY 126 and 150, respectively.

of $T1$ (Eq. (4)) were compared with the results using the fixed T value of 0.05. In each figure, the MODIS-based irrigated area overlaid the SAR irrigation map. By using the variable T, MODIS irrigated area expanded into areas with highly scattered paddy fields, which indicate that the variable T model is more robust in detecting irrigation of scattered small-scale paddy fields.

3.3. Evaluation of the variable T models

Agreement between the fixed T (0.05) model and three alternative Variable Threshold Models (Eqs. (4)–(6)) were evaluated with the SAR-based irrigated field maps (Fig. 6). The Variable Threshold Models performed much better than the fixed T models, with respective agreement rates of 40–94% and 34–86% for the SAR images of DOY 126 and DOY 150, in contrast with the 19–94% and 21–86% agreement rate for the fixed T model (Table 2). The variable T models overall showed better detection performance than the fixed T model for MODIS pixels containing few irrigated paddy fields (Fig. 6a and b), and in certain cases as much as doubled the detection rate.

On the other hand, the agreement rates decreased with EVI for both SAR images (Fig. 6c and d). All Variable Threshold Models showed similar agreement rates at low EVI levels, but the Variable Threshold Models were superior to the fixed T model with an EVI

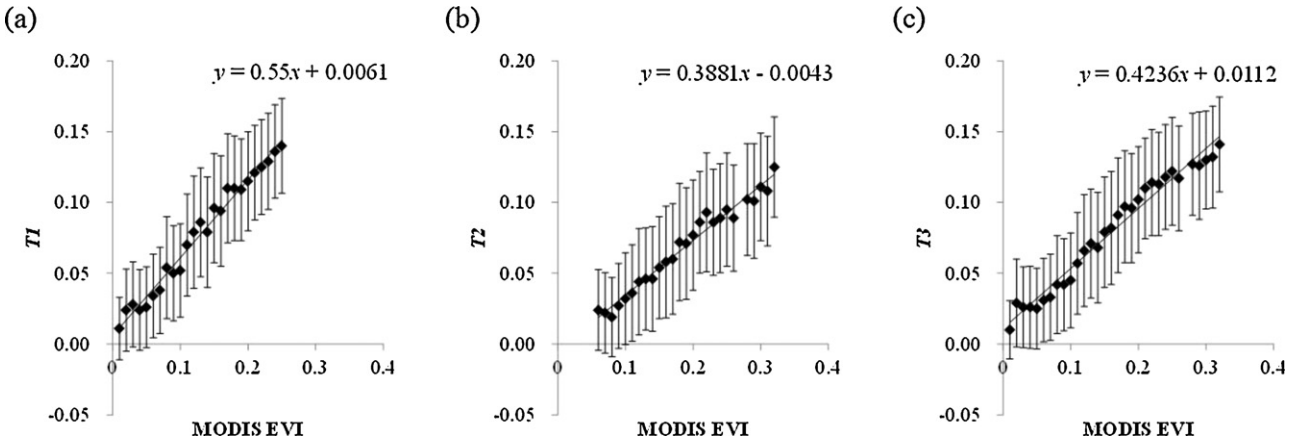

Fig. 4. Alternative Variable Threshold Models between T and EVI in DOY 126 (a), DOY 150 (b), and composed dates (c) in 2003. Solid diamond and error bars indicate mean values and a standard deviation at an interval of 0.01 EVI, respectively.

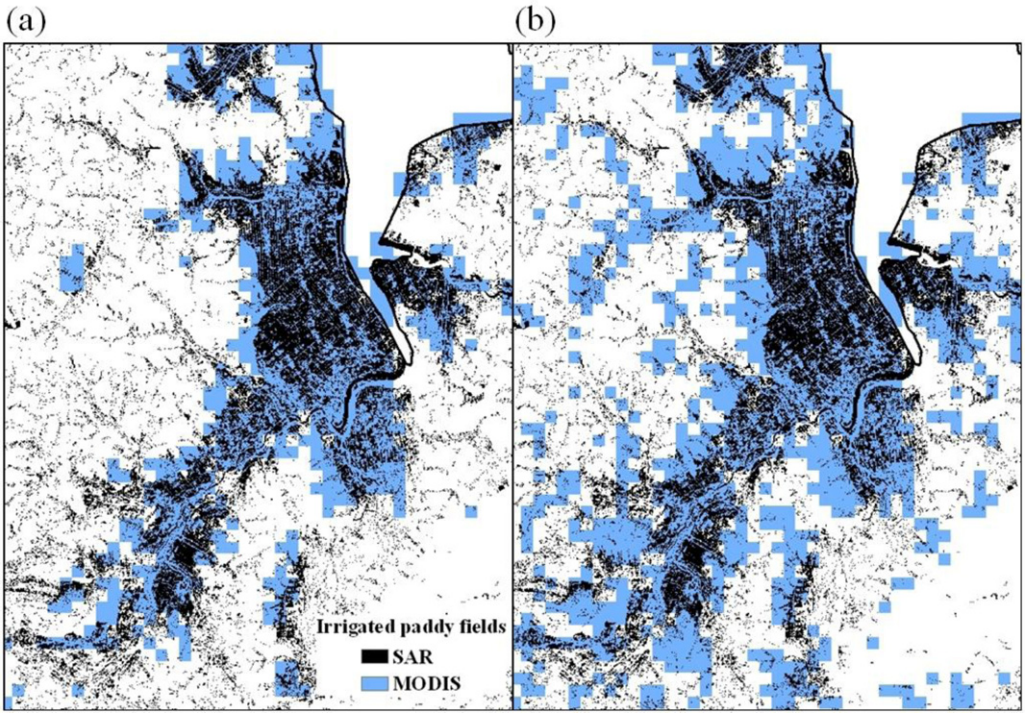

Fig. 5. Estimated spatial distribution of irrigated paddy rice fields using *T*0.05 (a) and *T*1 (b) in DOY 126, 2003.

range of 0.15 and higher. These results indicate that the Variable Threshold Model enhanced the detection performance of irrigated paddy fields where dry field sub-pixels are dominant. The enhanced detection performance was greater in early irrigation periods (DOY 126) than the latter ones (DOY 150). Overall, the *T*1 model showed the highest performance among the three Variable Threshold Models for both SAR image dates.

When applying the Variable Threshold Models, the estimated timing of irrigation dates were a few days earlier (−3.6 days) than those estimated by fixed *T* (*T*0.05) models (Table 3) but generally the differences were not appreciable within the MODIS 8-day data period. The detection of irrigation by the Variable Threshold Models for the Icheon 2 site is remarkable because the fixed model could not identify the irrigation at all. The threshold methods using *T*0.05, *T*1, *T*2, and *T*3 showed respective mean detection errors of +2.8, +0.1, +2.3, and +0.4 days with respect to the observations. Overall, the Variable Threshold Models detected irrigation dates for the 10 test sites with a mean error of 0.9 days, which was better than the error (+2.8 days) of the fixed threshold model (*T*0.05).

3.4. Mapping of irrigated paddy fields and timing of irrigation dates in Korea

The Variable Threshold Model identified more irrigated paddy field pixels (Fig. 7b) than the fixed *T* model (Fig. 7a). This is due to the capability of detecting irrigation for distributed small-scale paddy fields over heterogeneous land cover and complex terrain. Consequently, the *T*1, *T*2, and *T*3 models resulted in greater numbers (159,110; 150,936 and 151,740) of MODIS pixels identified as irrigated paddy fields than that (76,651) from the *T*0.05 model. Because of sub-pixel heterogeneity within a MODIS pixel and the presence of fallow paddy fields, direct comparison between the detected irrigated field area and the paddy field area from the National Land

Table 2
Agreement rates of MODIS detection of irrigated pixels with respect to number of irrigated sub-pixels from SAR images on DOY 126 and 150.

Count of irrigated pixel (SAR) DOY 126	Agreement (%)			
	*T*0.05	*T*1	*T*2	*T*3
1–100	19	40	37	37
101–200	48	60	60	61
201–300	64	68	70	71
301–400	78	80	82	82
401–500	88	89	89	89
501–625	94	93	94	93
Count of irrigated pixel (SAR) DOY 150	Agreement (%)			
	*T*0.05	*T*1	*T*2	*T*3
1–100	21	34	33	33
101–200	36	49	49	49
201–300	52	59	61	60
301–400	65	70	71	71
401–500	79	79	80	81
501–625	86	86	86	86

Table 3
Comparison of observed irrigation dates (DOY) and estimated irrigation dates from MODIS using *T*0.05 and developed *T* (*T*1, *T*2, and *T*3) in this study. N/A indicates that irrigation was not detected.

Site name	*T*0.05	*T*1	*T*2	*T*3	Observation
Chooncheon 1	120	118	117	117	120
Chooncheon 2	124	119	118	119	125
Icheon 1	127	123	124	123	117
Icheon 2	N/A	137	139	137	121
Ichoen flux	127	112	126	113	120
Hari flux	141	135	138	136	126
MASE 2001	113	111	112	111	113
MASE 2002	105	103	104	104	109
MASE 2003	109	107	108	107	114
MASE 2004	111	109	110	110	108
Mean error	+2.8[a]	+0.1	+2.3	+0.4	

[a] The error was averaged except for Icheon 2 where the irrigation was not detected.

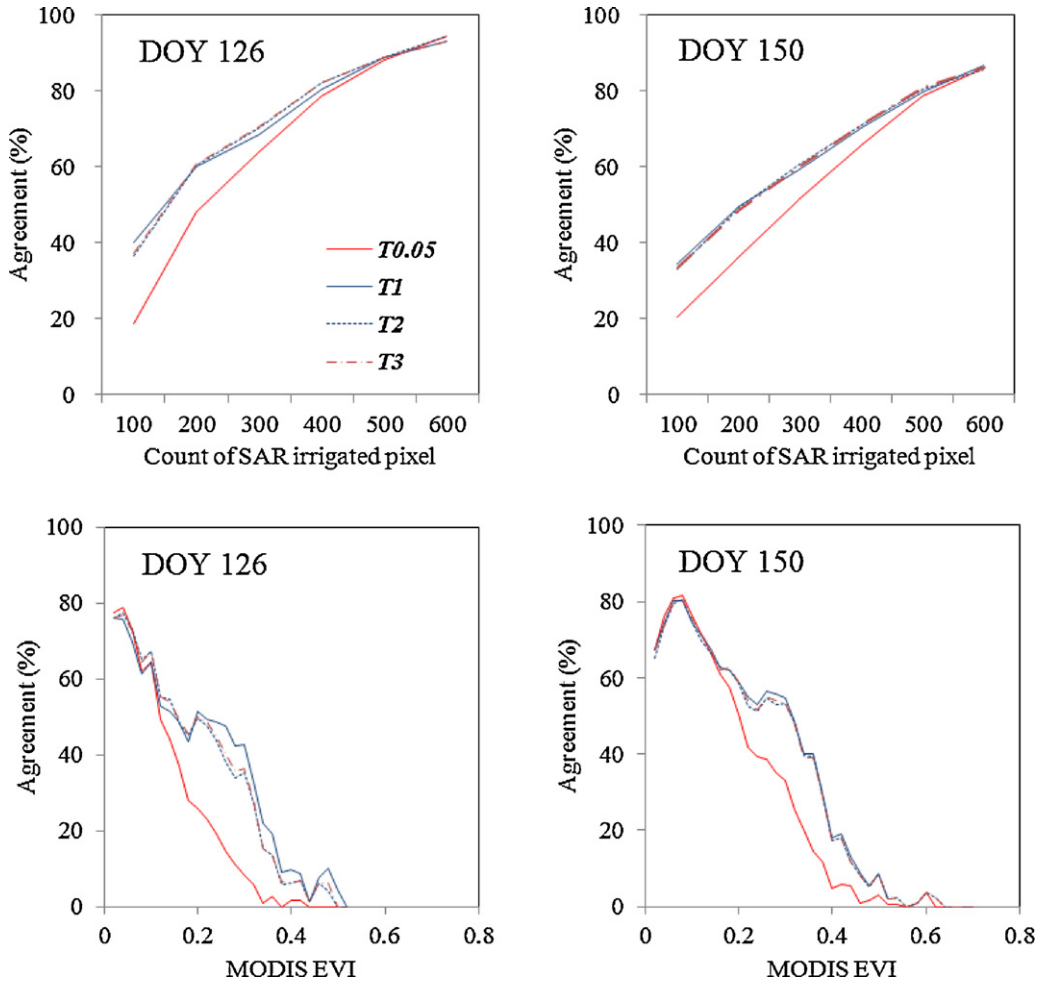

Fig. 6. Agreement rates (%) of MODIS-based detection of irrigated paddy rice fields with SAR-based irrigated paddy fields. The rate was plotted against counts of SAR-based irrigated sub-pixels within a MODIS 500 m pixel (a, b) and MODIS EVI (c, d) in DOY 126 and 150, respectively. *T*0.05 is used when applying a fixed threshold (0.05) and *T*1, *T*2, and *T*3 indicate the cases of Eqs. (4), (5), and (6), respectively.

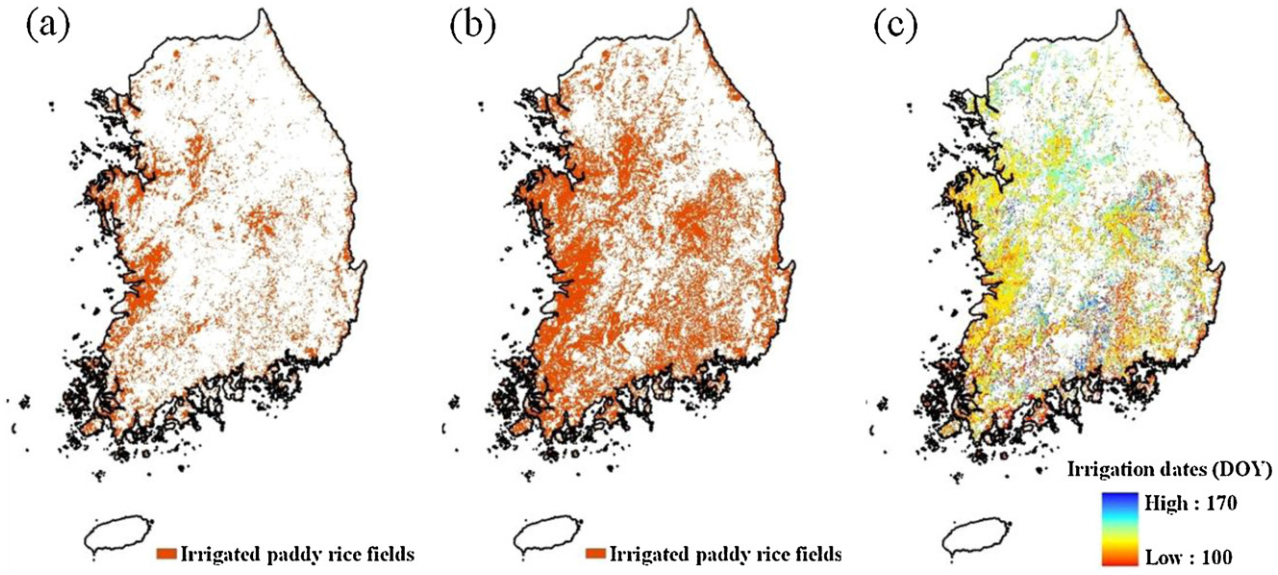

Fig. 7. Spatial distribution maps for MODIS-based irrigated fields, using threshold values of *T*0.05 (a) and *T*1 (b), and a map of timing of irrigation (c) in Republic of Korea, 2003.

Cover Map is less meaningful. Nevertheless, it is noteworthy that the Variable Threshold Model showed much less error (−27%) than the *T*0.05 model (−64%), when compared with number of paddy field pixels from the resampled 500 m National Land Cover Map.

The irrigation dates in 2003 varied from early April to mid June (Fig. 7c). In general, earlier irrigation was found in the southern than in the northern region, and more synchronized irrigation in larger plains (mostly located in the mid-west) compared to highly variable irrigation timing in small-scale paddy field areas. Higher elevation did not always result in later irrigation timing compared to the low-land plains and coastal areas.

4. Discussions and conclusions

The purpose of this study was to improve MODIS-based detection of irrigated area and irrigation timing, especially for distributed small-scale paddy field regions. Rather than using a fixed threshold value suggested by previous studies, we developed the Variable Threshold Model using different threshold values depending on MODIS EVI. This was based on a good linear relationship of MODIS EVI with the fraction of non-irrigated sub-pixels. The detection rate of the irrigated area obtained with the Variable Threshold Model was up to twice as high as that of the fixed threshold model, especially for the distributed small-scale paddy fields. In addition, The Variable Threshold Model showed less errors when compared to field observed irrigation dates.

Like many Asian countries, small-scale paddy fields in the Republic of Korea are usually located over a complex terrain. In the mountain regions, irrigation timing is less consistent than the large plains because irrigation systems are less developed and the irrigation timing is mostly based on the empirical knowledge of individual farmers. This study was able to detect those irregular irrigation dates in regions with a complex terrain.

Utilization of SAR images and well-defined land cover maps enabled us to obtain reliable information on the distribution of irrigated and non-irrigated paddy fields, as well as counts of different sub-pixels on paddy and dry fields and forests. This information provided critical baseline data to examine the effect of sub-pixel heterogeneity on MODIS spectral indices, leading to good linear relationships between MODIS EVI and the corresponding threshold values (Fig. 4). Such relationships enabled the development of alternative models using a variable threshold (Eqs. (4)–(6)).

For each SAR image date, different Variable Threshold Models (i.e. Eq. (4) versus Eq. (5)) were determined. Changed biophysical regimes on spectral reflectance from irrigated and non-irrigated landforms could partly explain the difference between Eqs. (4) and (5). As irrigation activity proceeds, both the irrigated sub-pixels and vegetation greenness in non-irrigated sub-pixels increase concurrently. Different spectral bands, however, show different responses to such changes in spectral environment. High sensitivity of shortwave infrared (SWIR) to surface water makes it useful in identifying water bodies from dry landforms, which causes a rapid change in LSWI even for a small body of sub-pixel irrigation within a coarse MODIS pixel. LSWI, however, does not change much with the changing amount of sub-pixel irrigation after the initial response, while EVI continuously increases with vegetation growth in dry and forest sub-pixels (Sun et al., 2009; Peng et al., 2011). The larger increase of EVI compared to LSWI can result in a higher threshold value relative to the same EVI at the later irrigation period as illustrated in Eq. (5). This implies that one should note the specific irrigation stage utilized for the development of a particular Variable Threshold Model, and be cautious in applying the model for the entire irrigation period. One of the possible solutions is to use multi-temporal SAR images to derive a more robust Variable Threshold Model as tested in this study.

Considerable variation in LSWI not related to paddy field irrigation were found in some circumstances: for example, in coastal regions it can be associated with sea salt aerosol containing high moisture, and in some regions, residual rain drops on leaf and soil surfaces after heavy rainfall events can affect the index. LSWI variations from such circumstances can sometimes meet, even temporarily, the detection criteria (i.e., $LSWI + T \geq EVI$) and hence, result in false classification to irrigated paddy fields. Our current approach did not take such cases into consideration, thus further improvements that consider such precedent rainfall events would be useful.

In conclusion, the Variable Threshold Models enhance detection performance on irrigated paddy fields especially for regions with distributed small-scale paddy fields. In this proposed approach, the sub-pixel heterogeneity was implicitly reflected and quantified through relationships between MODIS EVI and the threshold value. One of the shortcomings of this proposed approach is that it requires both more data (e.g., SAR images) and a reliable land cover map, compared to the previous approach using only MODIS images. Although the empirical threshold models are limited by temporal extrapolation for the whole irrigation periods, utilization of multi-temporal composite threshold models could mitigate this limitation. Further research is required to improve our method, especially considering precedent rainfall events and high-moisture aerosol effects.

Acknowledgements

This study was supported by the National Academy of Agricultural Science (PJ008546012012), RDA, Republic of Korea. The authors appreciate Lee and AsiaFlux Network for providing field irrigation observation data.

References

Bouvet, A., Toan, T.L., 2011. Use of ENVISAT/ASAR wide-swath data for timely rice fields mapping in the Mekong River Delta. Remote Sensing of Environment 115, 1090–1101.

FAOSTAT, 2001. Statistical Database of the Food and Agricultural Organization of the United Nations (FAO), Rome, Italy.

Gumma, M.K., Nelson, A., Thenkabail, P.S., Singh, A.N., 2011. Mapping rice areas of South Asia using MODIS multitemporal data. Journal of Applied Remote Sensing 5, 053547.

Huete, A.R., Liu, H.Q., Batchily, K., van Leeuwen, W., 1997. A comparison of vegetation indices global set of TM images for EOSMODIS. Remote Sensing of Environment 59, 440–451.

Huete, A., Didan, K., Miura, T., Rodriguez, E.P., Gao, X., Ferreira, L.G., 2002. Overview of the radiometric and biophysical performance of the MODIS vegetation indices. Remote Sensing of Environment 83, 195–213.

Islam, A.S., Bala, S.K., Haque, M.A., 2010. Flood inundation map of Bangladesh using MODIS time-series images. Journal of Flood Risk Management 3, 210–222.

Jeong, S., Jang, K., Hong, S., Kang, S., 2011. Detection of irrigation timing and the mapping of paddy cover in Korea using MODIS images data. Korean Journal of Agricultural and Forest Meteorology 13, 69–78.

Lee, H., 2006. Investigation of SAR Systems, technologies and application fields by a statistical analysis of SAR-related journal papers. Korean Journal of Remote Sensing 22, 153–174.

Lee, J., Lee, Y., Kim, G., Shim, K., 2005. CO_2 and water vapor flux measurement by Eddy covariance method in a paddy field in Korea. Korean Journal of Agricultural and Forest Meteorology 7, 45–50.

Moon, B., Hong, J., Lee, B., Yun, J.I., Park, E.W., Kim, J., 2003. CO_2 and energy exchange in a rice paddy for the growing season of 2002 in Hari, Korea. Korean Journal of Agricultural and Forest Meteorology 5, 51–60.

Ozdogan, M., Yang, Y., Allez, G., Cervantes, C., 2010. Remote sensing of irrigated agriculture: opportunities and challenges. Journal of Remote Sensing 2, 2274–2304.

Park, N., Lee, H., Chi, K., 2005. Feature extraction and fusion for land-cover discrimination with multi-temporal SAR data. Korean Journal of Remote Sensing 21, 145–162.

Peng, D., Huete, A.R., Huang, J., Wang, F., Sun, H., 2011. Detection and estimation of mixed paddy rice cropping patterns with MODIS data. International Journal of Applied Earth Observation and Geoinformation 13, 13–23.

Sakamoto, T., Nguyen, N.V., Kotera, A., Ohno, H., Ishitsuka, N., Yokozawa, M., 2007. Detecting temporal changes in the extent of annual flooding within the Cambodia and the Vietnamese Mekong delta from MODIS time-series imagery. Remote Sensing of Environment 109, 295–313.

Samad, M., Merrey, D., Vermillion, D., Fuchscarsch, M., Mohtadullah, K., Lenton, R., 1992. Irrigation management strategies for improving the performance of irrigated agriculture. Outlook on Agriculture 21, 279–286.

Sun, H., Huang, J., Huete, A., Peng, D., Zhang, F., 2009. Mapping rice paddy with multi-date moderate-resolution imaging spectroradiometer (MODIS) data in China. Journal of Zhejiang University-SCIENCE A 10, 1509–1522.

Uchida, S., 2007. Monitoring of paddy rice planting with complex cropping pattern using satellite remote sensing data—a case of West Java, Indonesia. In: Proceedings of the 28th Asian Conference on Remote Sensing (ACRS).

UNDESA, 2004. World population to 2300. United Nations Department of Economic and Social Affairs, Population Division (http://www.un.org/esa/population/publications/longrange2/WorldPop2300final.pdf).

Xiao, X., Boles, S., Frolking, S., Salas, W., Moore, B., Li, C., He, L., Zhao, R., 2002. Observation of flooding and rice transplanting of rice paddy fields at the site to landscape scales in China using vegetation sensor data. International Journal of Remote Sensing 23, 3009–3022.

Xiao, X., Boles, S., Liu, J., Zhuang, D., Frolking, S., Li, C., Salas, W., Moore, B., 2005. Mapping paddy rice agriculture in southern China using multi-temporal MODIS images. Remote Sensing Environment 95, 480–492.

Xiao, X., Boles, S., Frolking, S., Li, C., Jagadeesh, Y.B., Salas, W., Moore, B., 2006. Mapping paddy rice agriculture in South and Southeast Asia using multi-temporal MODIS images. Remote Sensing Environment 100, 95–113.